Hindawi
Geofluids
Volume 2017, Article ID 1683979, 17 pages
https://doi.org/10.1155/2017/1683979

Research Article

Effect of Water Saturation on the Diffusion/Adsorption of ^{22}Na and Cesium onto the Callovo-Oxfordian Claystones

Sébastien Savoye,[1] Serge Lefevre,[1] Agnès Fayette,[1] and Jean-Charles Robinet[2]

[1]*DEN-Service d'Etude du Comportement des Radionucléides (SECR), CEA, Université Paris-Saclay, 91191 Gif-sur-Yvette, France*
[2]*R&D Division, Transfer Unit, Andra, 92298 Châtenay-Malabry, France*

Correspondence should be addressed to Sébastien Savoye; sebastien.savoye@cea.fr

Received 29 May 2017; Revised 7 September 2017; Accepted 31 October 2017; Published 17 December 2017

Academic Editor: Douglas K. Solomon

The diffusion and adsorption behaviors of sodium and cesium were investigated in the Callovo-Oxfordian claystones (France) under unsaturated conditions. Through-, out-, and in-diffusion laboratory experiments were performed on intact and compacted samples. These samples were partially saturated using an osmotic method for imposed suction up to 9 MPa. This specific technique enabled us to obtain water saturation degree ranging from 81% to 100% for intact samples and from 70% to 100% for compacted materials. The results showed a very low impact of water saturation on the extent of adsorption for ^{22}Na and cesium, onto intact and compacted materials. Such observations suggest that the saturation degrees were not low enough to limit the access of cations to adsorption sites on clay surfaces. At full saturation, enhanced diffusion for ^{22}Na and cesium was clearly evidenced onto intact and compacted samples. Under unsaturated conditions, the diffusion behavior for Cs and ^{22}Na was not only slower but also distinct as compared to fully saturated samples. For the intact rock and under suction of 1.9 MPa, the Cs diffusivity was reduced by a factor of 17, whereas for sodium, it was reduced by a factor of 5. Explanation was then proposed to explain such a difference.

1. Introduction

Geological clayey formations are being widely investigated by several countries in the world for hosting radioactive waste disposal facilities [1, 2]. Due to their very low permeability such rocks limit the radionuclide transfer by very slow diffusive process. Moreover, the clay minerals present within these rocks are capable of strongly adsorbing cationic radionuclides. Therefore, both of these properties could slow down radionuclide migration towards the biosphere.

However, there are several cases where the soils or rocks surrounding such waste disposal facilities can be unsaturated, leading to a potential change of their containment properties. For example, many landfills are constructed in arid or semiarid environments, where the soil can be unsaturated at great depths [3]. In the case of deep argillaceous formations such as the Callovo-Oxfordian claystones studied by the French Waste Management Agency (Andra), the presence of a radioactive waste disposal facility is expected to induce hydraulic disequilibrium in the near-field of the host-rocks. During the construction and the operation phases ventilation of the underground drifts and shafts could partially dehydrate the rock around these structures [1, 4]. And, after resaturation phase, the hydrogen produced by canister corrosion would further lead to partial dehydration of rocks [5]. Hence, in this context it is important to understand how unsaturated conditions can impact radionuclide migration through these formations, that is, in terms of diffusion and adsorption processes.

However, it is a known fact that through water-saturated low permeability clay rocks, performing diffusion/retention experiments is already a challenging task (e.g., [2, 6, 7]). Also, in literature, only a few diffusion/retention experiments have been carried out under partially saturated conditions. Most of these experiments used half-cell method [8–11], known to generate artifacts because of partial contact between the two half-cells [12]. Thus, to find an alternative, in recent times we presented an innovative technique. This technique allows the diffusion of uncharged tritiated water (HTO) and solutes through unsaturated Callovo-Oxfordian (COx)

claystones [13, 14]. But it can be also applied to compacted materials with variable clay content [15]. Contrary to half-cell method, here the targeted water saturation degree is imposed by osmosis process. This can then be combined with through-diffusion method to determine the diffusive behavior of HTO and anionic species ($^{125}I^{-}$). This osmotic technique can further be combined with decreasing source concentration method or transient in-diffusion method to determine diffusion/adsorption of cesium (see [12] for details about these techniques).

The previous results obtained in our studies under partially saturated conditions revealed a very sharp decrease of the effective diffusion coefficients (D_e), especially for cesium. For instance, when dehydrating intact COx samples down to 81% of saturation, the D_e values were reduced by a factor of 7 for HTO, by a factor of 50 for iodide, and by a factor of about 60 for cesium. The cesium diffusivity decreased by an order of magnitude higher than the decrease observed for tritiated water (HTO). This behavior was still unexplained, since cesium and HTO were expected to diffuse through the same volume of the pore space, in fully saturated claystones. Therefore, two hypotheses had been proposed to explain such an unexpected difference. First, under partially saturated conditions HTO diffusion could occur both in liquid and vapor phases. Solutes such as cesium would have been forced to diffuse in only liquid phase. This hypothesis can thus explain the observed drop in available diffusive pathway for Cs ions as the sample moves from saturated to partially saturated conditions. The inhibition of surface diffusion in dehydrated pores and resulting reduced diffusion were the base for our second hypothesis. This hypothesis also has valid stand as surface diffusion has been evoked to explain the too high cation flux in fully saturated conditions, compared to what can be predicted from a simple pore diffusion model using water diffusion coefficient [16–18]. Therefore, if we go by the convention of second hypothesis, it is clear that, as the dehydration increases, the clay surface accessible for surface diffusion decreases. This phenomenon could thus explain enhanced diffusion in fully saturated conditions and slow diffusion in partially saturated conditions for Cs ions.

In order to address this issue, the present study aims to properly determine the extent of the diffusive/adsorption behavior of two cations (i.e., ^{22}Na and cesium) onto partially saturated claystone samples under intact or compacted state. In this study, ^{22}Na was chosen because it is a weakly adsorbed cation, known to be less impacted by surface diffusion mechanisms than cesium at full saturation [16–18]. Thus its diffusive behavior is expected to be "intermediate" between cesium and HTO. Moreover, the purpose of using intact and compacted samples is twofold: (i) to verify if the extent of adsorption under partial water-saturated conditions is consistent with fully saturated conditions (see [19] for adsorption of cesium onto full-saturated Callovo-Oxfordian claystones) and (ii) to investigate the role played by the pore network geometry on diffusion.

In this view, we used several diffusive techniques in order to acquire both the effective diffusion coefficients and the extent of cation adsorption. The experimental conditions were identical to those previously used in Savoye et al. [13, 14]: (i) rock samples issued from a core in the immediate vicinity and (ii) use of the same four suction values (up to 9 MPa) generated by osmosis process. The cationic adsorption values were acquired using the principle of the diffusive method developed by Montavon et al. [20]. However, in our case this method was adapted to partially saturated conditions. The cationic equilibrium between rock and reservoir was achieved using decreasing source concentration method. And, at the end of the experiment, cation concentration was measured within rock sample by means of abrasive peeling technique developed by Van Loon and Eikenberg [21]. In addition to this "in-diffusion until equilibrium" method, through- and out-diffusion techniques were also used for investigating the diffusion of ^{22}Na through intact rock samples. All these experiments enabled us to obtain a direct comparison of the diffusive/adsorption behavior of two types of cations (sodium and cesium) as a function of the saturation degree.

2. Materials and Methods

2.1. Sample Origin and Sample Preparation. The rock samples used for the measurements originated from Callovo-Oxfordian sedimentary formation (COx) located in eastern part of Paris basin. The Callovo-Oxfordian (COx) formation has been selected by France to host a deep underground nuclear waste repository and currently studied by Andra in Meuse/Haute Marne Underground Research Laboratory (URL). The mineralogy of COx is mainly composed of clay minerals (illite, illite/smectite mixed-layered mineral, chlorite, and kaolinite), quartz, and carbonates [22]. The core sample referenced EST27340 (484.5–484.8 m bgl) was selected for this study. This core originated from an upward drilling cored from the main shaft of the Meuse/Haute Marne URL (490 m bgl). This core is located at an immediate vicinity of the core studied by Savoye et al. [13, 14] for determining the diffusive behavior of HTO, ^{125}I, and Cs through intact partially saturated claystone samples. The mineral and microstructural properties of these two cores are expected to be very similar, thus leading to comparable diffusion/adsorption properties.

To study the intact materials, eight samples were sliced from EST27340 core using a diamond wire saw (no lubricating fluid was used). These slices were cut in such fashion so that diffusion would be perpendicular to the bedding planes. Out of eight samples, four samples were dedicated to ^{22}Na through- and out-diffusion experiments. These selected slices were then placed on a lathe to obtain 36-mm diameter disks. The remaining four slices were dedicated to "in-diffusion until equilibrium" experiments and petrophysical measurement. They were placed on a lathe to obtain 18.75-mm-diameter disks. Moreover, to study compacted materials, pieces of EST27340 core were crushed and sieved (100 μm mesh). All of the sliced samples and powder were stored at 30.0 ± 0.2°C in desiccators containing a NaCl-oversaturated solution (suction = 39 MPa), until suction equilibrium. This equilibrium was achieved after *ca.* 3 months

Table 1: Summary of the samples, the tracers, and the type of experiments performed in this study. √ means performed.

Sample state	Thickness (mm)	[PEG] (g/g of solution)	Applied suction (MPa)	Type of experiments			
				Through-diffusion	Out-diffusion	In-diffusion until equilibrium	Petrophysical measurement
Intact	11.13	0	0	$^{22}Na^{+}$	√		
Intact	11.16	0.42	1.9	$^{22}Na^{+}$	√		
Intact	10.96	0.76	6.3	$^{22}Na^{+}$	√		
Intact	11.15	0.95	9	$^{22}Na^{+}$	√		
Intact	6.01	0.95	9			$^{22}Na^{+}$	
Compacted	10.17	0	0			$^{22}Na^{+}$	
Compacted	9.75	0.42	1.9			$^{22}Na^{+}$	
Compacted	9.88	0.76	6.3			$^{22}Na^{+}$	
Compacted	9.93	0.95	9			$^{22}Na^{+}$	
Intact	8.60	0	0			$[Cs]_{ini} = 8.7 \times 10^{-4}$ M	
Intact	2.08	0.95	9			$^{134}Cs + [Cs]_{ini} = 7.6 \times 10^{-4}$ M	
Compacted	6.03	0	0			$^{134}Cs + [Cs]_{ini} = 8.4 \times 10^{-4}$ M	
Compacted	3.93	0.42	1.9			$^{134}Cs + [Cs]_{ini} = 7.6 \times 10^{-4}$ M	
Compacted	4.02	0.76	6.3			$^{134}Cs + [Cs]_{ini} = 8.4 \times 10^{-4}$ M	
Compacted	3.88	0.95	9			$^{134}Cs + [Cs]_{ini} = 7.8 \times 10^{-4}$ M	
Intact	8	0.95	9				√
Compacted	10.09	0	0				√
Compacted	10.11	0.42	1.9				√
Compacted	9.86	0.76	6.3				√
Compacted	10.09	0.95	9				√

(indicated by mass stabilization). The Callovo-Oxfordian powder was then directly compacted into the in-diffusion cells at a dry density of 1.6 g cm^3. The dry density of intact COx sample was equal to 2.19 ± 0.20 g cm^{-3} as determined by Savoye et al. [13]. Note that for the "in-diffusion until equilibrium" experiments, the sample thickness was adapted within range of 10 mm to 2 mm in order to minimize the achievement of the equilibrium state. And for samples dedicated to through- and out-diffusion and petrophysical measurements, the adapted thickness was about 1 cm-thick (see Table 1).

2.2. Desaturation Procedure. The osmotic technique consists of inducing suction by generating an osmosis process between pore water (present in the pores of the sample) and aqueous solution of large sized molecules of polyethylene glycol (PEG; for more details see [13]). For this reason, the sample surface is separated from the PEG solution using a semipermeable membrane (which is permeable to all except PEG). Thus the generated osmotic suction allows sample to be kept under unsaturated conditions. Moreover, Delage et al. [23] demonstrated that the value of imposed suction and the resulting saturation state of sample purely depend on the concentration of PEG in solution. For this reason, in present study, just by gradual increment of PEG concentrations (0, 0.42, 0.76, and 0.95 g per g of solution), we obtained gradual increase in generated suction values (0, 1.9, 6.3, and 9 MPa, resp.) [13–15]. At each suction value, thus, a desired saturation state was achieved. Note that semipermeable membranes with 3500 g mol^{-1} molecular weight cut-off (MWCO) were chosen in order to prevent the PEG 6000 (i.e., 6000 g mol^{-1} molecular weight) from bypassing the membranes.

For osmotic resaturation, synthetic solutions were prepared with ultrapure deionised water (18.2 MΩ cm^{-1}), PEG 6000 (Merck, Germany), and commercial salts (American Chemical Society reagent grade or higher quality and purity salts), so as to obtain a chemical composition as close as possible to pore water and to limit as much as possible any chemical disturbance. The recipe to mimic pore water condition was based on the chemical composition measured from in situ water sampling performed at a level close to the sampling level of this study (475 m bgl) [24]. The

total concentrations for calcium, magnesium, potassium, and sodium were 3.0, 2.0, 1.7, and 51.6 mmol L^{-1}, respectively. The anion concentrations for chloride, sulfate, and the carbonate species were 41.0, 11.0, and 0.70 mmol L^{-1}, respectively. Note that since no PEG can diffuse into the pores of the samples owing to the presence of the semipermeable membrane, mmol L^{-1} means mmol per liter of synthetic pore water without PEG.

2.3. Experimental Setups. Two distinct experimental setups were used for performing either through- and out-diffusion experiments on 36-mm-diameter intact samples or "in-diffusion until equilibrium" on 18.75-mm-diameter intact and compacted samples.

The first setup is the same as the setup developed by Savoye et al. [13] for studying through-diffusion of HTO through partially saturated Callovo-Oxfordian claystones. This setup comprises a diffusion cell in which the sample is held, connected to two reservoirs (the upstream and downstream reservoirs) by tubes, and a peristaltic pump (IPS, Ismatec, Idex Corporation, USA) allowing both solutions to circulate from each side of the cell to their corresponding reservoir. The protocol used for holding the 36-mm-diameter sample inside the diffusion cell is as follows: the sample was inserted in a stainless-steel holder and was sandwiched between two semipermeable membranes made of cellulose acetate (Spectra-Por 3500 Da, Spectrum Laboratories, USA). Afterwards, two polyetheretherketone (PEEK) grids (Polyetheretherketone Mesh, Goodfellow, England) with 60 and 45 meshes were placed between the o-rings to limit the dead volume. Then, two end-pieces were placed in position on both sides. See Figure 1 in Savoye et al. [13] for details about the setup. Note that no filter was required under this experimental configuration. During the hydric equilibrium phase, both sides of sample were in contact with the same synthetic pore water plus PEG, using a unique reservoir.

The second setup used for the "in-diffusion until equilibrium" on 18.75-mm-diameter intact and compacted samples is based on a different principle since the sample holder is directly immersed into a source reservoir containing a solution homogenized by means of a magnetic stirrer. Into the holder made of PEEK, the sample was also sandwiched between two semipermeable membranes but two stainless-steel filters were used to keep sample within cell. See Figure 65 in Altmann et al. [25] for a detailed description of this setup. Note that in this case, tracer diffusion occurs on both sides of the sample.

Note that the thickness of the semipermeable membranes is less than 100 μm and the weak influence of such membranes on diffusion was demonstrated by means of the comparison between diffusion results obtained at full saturation from setups equipped or not with these membranes. See, for instance, Savoye et al. [13], Table 2, where D_e (HTO) values are equal to 2.3×10^{-11} m^2 s^{-1} and 2.2×10^{-11} m^2 s^{-1} with and without membranes, respectively.

Before starting either the dismantling of the cells for performing the petrophysical measurements or the diffusion tests (described below), the hydric equilibrium for the rock sample was assumed to be achieved after one month based on the work done by Savoye et al. [13].

2.4. Petrophysical Measurements. In order to determine the water content and degree of saturation as a function of imposed suction, petrophysical measurements have been performed as follows: (i) water contents (w) were measured (i.e., weighed) before and after oven-heating at 105°C for 48 h and were described on a mass basis relative to the wet mass; (ii) bulk dry density ρ_d was determined by measuring the pressure exerted by the sample immersed in kerosene according to Archimedes' principle [26]; (iii) grain density was determined in a Micromeritics Accupyc 1330 helium pycnometer.

The volumetric moisture content, θ, is calculated from the water content using the following expression [27]:

$$\theta = \frac{w \times \rho_s}{(1 - w) \times \rho_w + w \times \rho_s}, \quad (1)$$

where ρ_w is the density of the pore water (1 g cm^{-3}) and ρ_s is the measured grain density of the rock ((2.7023 ± 0.0016) g cm^{-3}, [13]).

Moreover, the total porosity is deduced from the following equation:

$$\phi = 1 - \frac{\rho_{\text{bulk, dry}}}{\rho_s}. \quad (2)$$

Finally, the saturation degree (S_w) corresponds to the ratio of volumetric water content (θ) over total porosity (ϕ). Note that no petrophysical measurement was carried out on samples contaminated by radiotracers due to radiological constrains. Therefore, for the series dedicated to "in-diffusion until equilibrium" into compact or intact samples, supplementary samples were specifically dedicated to petrophysical measurements. For the series dedicated to ^{22}Na diffusion experiments through intact samples, we assumed that these radioactive samples were at the same saturation degrees as their neighbor samples previously studied by Savoye et al. [13] under the same experimental conditions.

2.5. Protocols for the Diffusion Experiments. After one month of saturation treatment, through- and out-diffusion experimental cells were connected to two distinct reservoirs. The upstream reservoir was filled with 92 cm^3 of synthetic pore water (excluding the volume of PEG), labelled with ^{22}Na, and a 20-cm^3-downstream reservoir filled with synthetic pore water without tracer was connected to the cell. The ^{22}Na injected activity was 2.95 MBq L^{-1} for cell at 0 g of PEG and 4.8 MBq L^{-1} of synthetic pore water without PEG for three other diffusion cells. During the through-diffusion step, the solution in the downstream reservoir was regularly replaced in order to maintain the lowest tracer concentration as reasonably possible, that is, less than 3% of the one measured in the upstream reservoir.

However, the upstream reservoir concentration was left to freely decrease over the total experimental time. The completion of through-diffusion stage was followed by an

out-diffusion procedure. This step was applied to study the reversibility behavior of ^{22}Na diffusing out of the rock sample. The solutions in both of the reservoirs were completely replaced by synthetic pore water without tracer to allow ^{22}Na to diffuse out of the rock samples. At selected time intervals, the ^{22}Na activity in the solutions was measured for monitoring the activity rate at which the tracers out-diffused from the samples (see [13] for details).

The cell reservoirs dedicated to "in-diffusion until equilibrium" experiments were filled with synthetic pore water labelled with either ^{22}Na (with an activity of about 1.75 MBq L^{-1}) or ^{134}Cs (with an activity of about 1.25 MBq L^{-1}) and CsCl at $8 \cdot 10^{-4}$ mol L^{-1}. Assuming a K_D value of 26 L kg^{-1} (see (8) below) estimating from Savoye et al. [14], this CsCl concentration was selected to ensure that equilibrated concentration is close to $5 \cdot 10^{-4}$ mol L^{-1}. Moreover, as cesium has higher affinity compared to ^{22}Na towards the rock sample, a larger solution volume of 0.11 L of synthetic pore water without PEG was chosen (for ^{22}Na 0.03 L of synthetic pore water without PEG). At selected time intervals, the activity in the solutions was measured for determining the achievement of the equilibration. When this condition is achieved, the diffusion cells were dismantled and the rock samples were dried at 105°C for 24 h. Then, the ^{22}Na and ^{134}Cs profiles in rock were acquired using a high-resolution abrasive peeling method developed by Van Loon and Eikenberg [21]. The principle of this technique is the removal of thin layers of rock sample by abrading the material on grinding paper. This abraded powder is then recovered by water leaching. The leached solution is then transferred into a tube directly used for γ counting. Note, after each successive abrasion, the sample thickness was measured using a micrometer (Mitutoyo, Japan).

^{22}Na and ^{134}Cs activities were counted by γ counter (Packard 1480 WIZARD, USA). ^{22}Na and ^{134}Cs data were corrected for radioactive decay with respect to the tracer injection time. A summary of the samples, the types of the experiment, and studied species is reported in Table 1.

2.6. Treatment of Experimental Results. The analysis of through- and out-diffusion experiments for ^{22}Na was based on Fick's second law for one-dimensional transport:

$$\frac{\partial C}{\partial t} = \frac{D_e}{\alpha}\frac{\partial^2 C}{\partial x^2} = \frac{D_e}{\varepsilon_a + \rho_d K_D}\frac{\partial^2 C}{\partial x^2}, \tag{3}$$

where C is the concentration or activity per volume unit in the solute phase (mol m^{-3} of synthetic pore water without PEG or Bq m^{-3}); t, the time (s); D_e, the effective diffusion coefficient (m^2 s^{-1}); ε_a, the diffusion-accessible porosity (m^3 m^{-3}); ρ_d, the bulk dry density (kg m^{-3}); K_D, the distribution coefficient (L kg^{-1}).

The K_D value was calculated from the relationship $K_D = (\alpha - \varepsilon_a)/\rho_d$ and by assuming that the accessible porosities of ^{22}Na were identical to volumetric moisture content; that is, $\varepsilon_a = \theta = \phi \cdot S_w$. *Thus,* for interpretation of ^{22}Na diffusion experiments, D_e and K_D were adjusted parameters and ε_a and ρ_d were considered as input parameters.

For through-diffusion system used for ^{22}Na, boundary and initial conditions are as follows:

$$\begin{aligned} C(x,t) &= 0, \quad t = 0, \\ C(x,t) &= C_0, \quad x = 0,\ t = 0, \\ C(x,t) &= 0, \quad x = L,\ t > 0, \end{aligned} \tag{4}$$

where L is the sample thickness (m) and C_0 is the initial concentration of tracer in the upstream reservoir (mol m^{-3} of synthetic pore water without PEG or Bq m^{-3} of synthetic pore water without PEG). Fully analytical solutions for through-diffusion and reservoir-depletion studies are obtained in the Laplace space and they can be found in Didierjean et al.'s [28] paper. Afterwards, they were subsequently numerically inverted to provide the solution in time [29].

For out-diffusion stage, (3) has to be solved with the corresponding boundary conditions:

$$C(0,t) = C(L,t) = 0, \quad t > 0. \tag{5}$$

Moreover, we can assume a linear concentration gradient across the sample when through-diffusion stage reaches steady-state. The concentration profile at this stage provides the initial out-diffusion conditions and is mathematically expressed as

$$C(x) = C_{\text{TD\_end}}\left(1 - \frac{x}{L}\right), \tag{6}$$

where $C_{\text{TD\_end}}$ is the concentration of tracer in upstream reservoir at the end of through-diffusion step (mol m^{-3} of synthetic pore water without PEG or Bq m^{-3} of synthetic pore water without PEG).

According to Jakob et al. [30], the total amount of tracer (mol or Bq) diffused out of the sample at the two boundaries is given by

$$\begin{aligned} A(0,t) &= 2 \cdot C_{\text{TD\_end}} \cdot S \cdot \alpha \\ &\quad \cdot L\left[\frac{1}{6} - \sum_{n=1}^{\infty}\frac{1}{\pi^2 n^2} e^{-((n\cdot\pi)/L)^2\cdot(D_e/\alpha)\cdot t}\right], \\ &\qquad\qquad \text{at } x = 0, \\ A(L,t) &= 2 \cdot C_{\text{TD\_end}} \cdot S \cdot \alpha \\ &\quad \cdot L\left[\frac{1}{12} + \sum_{n=1}^{\infty}\frac{(-1)^n}{\pi^2 n^2} \cdot e^{-((n\cdot\pi)/L)^2\cdot(D_e/\alpha)\cdot t}\right], \\ &\qquad\qquad \text{at } x = L, \end{aligned} \tag{7}$$

where S is the surface of the rock sample (m^2).

A different approach however was used for interpretation of "in-diffusion until equilibrium" experiments. In these experiments, equilibrium is assumed to be between solution and solid phase. Thus, by determining the rock concentration using abrasive peeling and final concentration in the solution, one can use the following relationship to estimate the distribution coefficient, K_D:

$$K_D = \frac{C_{\text{solid}}}{C_{\text{eq\_solution}}}, \tag{8}$$

where C_{solid} is the concentration of tracer adsorbed on solid (mol kg^{-1} of dry sample) and $C_{eq\_solution}$ is the final concentration of tracer remaining in solution (mol L^{-1} of synthetic pore water without PEG).

Therefore, using these K_D values as input parameters, the D_e values were estimated by applying the Fick's second law using the following initial and boundary conditions:

$$\begin{aligned} C(x,t) &= 0, \quad t = 0, \\ C(x,t) &= C_0, \quad x = 0,\ t = 0, \\ \frac{\partial C}{\partial x} &= 0 \quad x = \frac{L}{2} + l,\ t \geq 0, \end{aligned} \tag{9}$$

where L and l are the sample and filter plate thicknesses (m), respectively.

In order to take into account the presence of filter plate, fully analytical solution was only obtained in Laplace space (see [28] for finding this solution). This solution was subsequently numerically inverted to provide the solution in time [29]. In this case, the following input parameters were used for filter plate: thickness, 1.95 mm; filter plate geometry factor, D_0/D_e = 8.19 given by Descostes et al. [31]; porosity, 37%; D_0, self-diffusion coefficients for Na and Cs from Savoye et al. [32] (i.e., 1.18×10^{-9} m^2 s^{-1} and 1.74×10^{-9} m^2 s^{-1}, resp.).

Note that the viscous PEG solutions cause difficult interpretation of results since the change imposed on diffusive properties of filter plate is difficult to estimate. Therefore, for the associated D_e values, only in-diffusion experiments carried out without PEG were extensively discussed in this study. A rough D_e estimation was however performed from other experiment data with PEG. Here it was assumed that the diffusive properties of filter plates were the same as in the cases without PEG. This is because of homogenization of PEG solutions by means of magnetic stirrer. The associated D_e values are only reported in Figures 4, 5, 6, and 7 for information.

Finally, the uncertainties on experimental data were estimated by propagation of analytical error variances (σ^2_{V1}, σ^2_{V2}, etc.) following the Gaussian error propagation law. The adopted approaches used for determining the uncertainties on experimental data and error range of the diffusive parameters are described in Savoye et al. [33].

3. Results

3.1. Petrophysical Data. Figure 1 shows the saturation degree evolution as a function of the imposed suction on compacted materials and on intact rock samples. The suction up to 9 MPa allowed the intact samples to be dehydrated down to 81% and the compacted samples down to 70%. Note that a good consistency of the saturation degrees was determined on intact rock samples at the highest suction by Savoye et al. [13] and in the present study. Moreover, at each suction level strictly higher than 0 MPa, compacted materials display saturation degree values about 10% lower than the ones measured on intact materials. In comparison to intact rock, the pore size distribution in compacted materials at ρ_d equal to 1.6 g cm^{-3} is characterized by larger pore diameters (see, e.g., Figure 9 in [34]). Consequently, in agreement with the Jurin-Laplace's law, a lower saturation degree is expected in compacted materials for the same suction. However, one issue that needs to be addressed is to know whether dehydration is able to limit the accessibility of cations present in pore water to clay surfaces (including interlayer space).

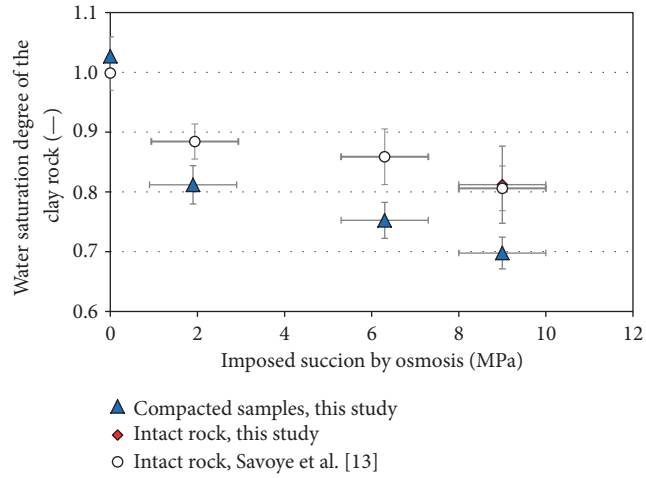

Figure 1: Values of degree of saturation determined on rock samples having undergone the osmotic method as a function of the imposed suction.

3.2. ^{22}Na Diffusion Experiments. Figures 2(a) and 2(b) show the normalized activity in upstream reservoir and the normalized instantaneous flux in downstream reservoir for four through-diffusion experiments performed with ^{22}Na on intact clay rocks (S_w = 81, 86, 89, and 100%). Here, the normalized activity in upstream reservoir is the ratio of ^{22}Na activity over the initial ^{22}Na activity. Whereas the normalized instantaneous flux in m s^{-1} is the ratio of instantaneous flux in Bq m^{-2} s^{-1} over the concentration in upstream reservoir in Bq m^{-3}. The effect of desaturation is (i) to retard the activity decrease in upstream reservoir and (ii) to decrease the incoming instantaneous flux in downstream reservoir, compared to full-saturated sample. For example, incoming flux decreases by a factor of approximately 20 for ^{22}Na from full saturation to 81% of saturation.

Interpretation of such dataset is classically achieved using a least square fitting of the model for both the incoming flux in downstream reservoir and the activity decrease in upstream reservoir. However, such approach is only applicable to through-diffusion experiment carried out in fully saturated sample (Figure 2). The associated diffusive parameters are listed in Table 2. For partially saturated samples, the simulated curves were calculated from incoming flux only (solid lines). This estimation however underestimated the activity decrease in upstream reservoir (Figure 2(a)). Also the higher the desaturation is, the larger the discrepancy is. This suggests that more of ^{22}Na would diffuse into partially saturated samples than expected from ^{22}Na diffusing out

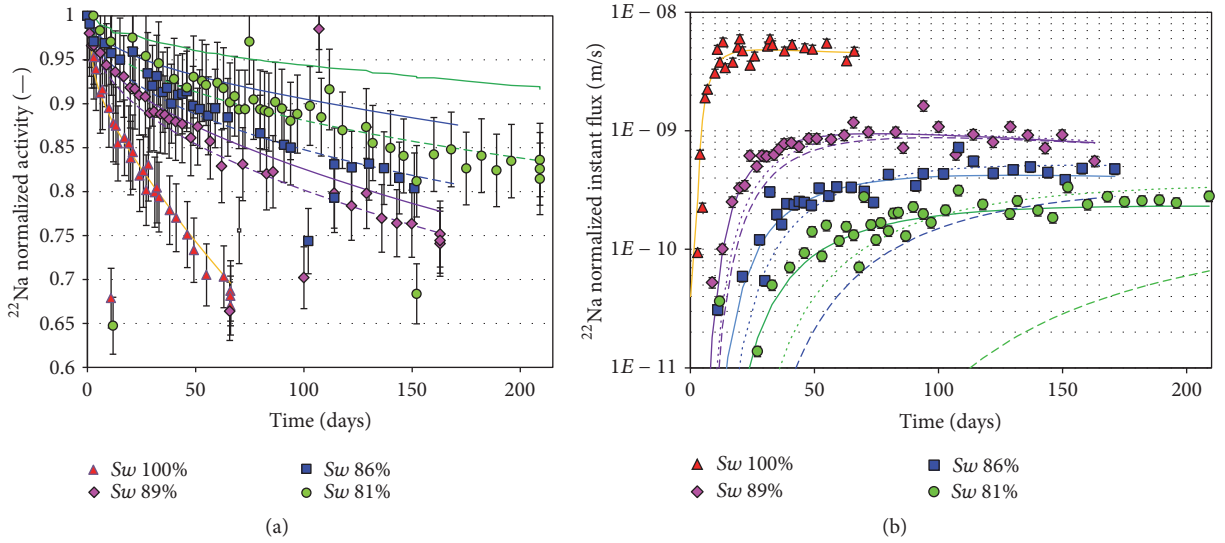

Figure 2: Evolution of the ^{22}Na activity in the upstream reservoir (a) and ^{22}Na normalized instantaneous fluxes (b) at different values of degree of saturation for intact materials. The solid curves were calculated using the semianalytical solutions with the parameters specified in Table 2 from the incoming flux data. The dotted curves were calculated from activity evolution data in upstream using the same D_e values as the ones calculated from the incoming fluxes. The dashed curves were calculated from activity evolution data in upstream adjusting D_e values so as to prevent the simulated incoming flux from being higher than the experimental one. Decay corrections were applied with respect to the start of the through-diffusion stage.

Table 2: Values of distribution coefficient (K_D) and effective diffusion coefficient (D_e) for the though- and out-diffusion for ^{22}Na for various imposed suction values on intact materials. Values between brackets indicate the uncertainty ranges.

Sample state	Species	Diffusion method	Saturation degree (%)	K_D (mL g^{-1})	$D_e \times 10^{-11}$(m^2 s^{-1})
Intact	$^{22}Na^+$	Through-diffusion, incoming flux & upstream	100	0.79 (0.53–0.90)	4.85 (3.80–5.80)
Intact	$^{22}Na^+$	Out-diffusion upstream	100	0.70 (0.60–0.76)	5.50 (5.0–6.0)
Intact	$^{22}Na^+$	Out-diffusion downstream	100	0.75 (0.60–0.77)	5.50 (5.0–7.0)
Intact	$^{22}Na^+$	Through-diffusion, incoming flux	89	0.78 (0.55–0.88)	1.4 (1.35–1.45)
Intact	$^{22}Na^+$	Through-diffusion, upstream	89	0.94–1.14	1.4–1.50
Intact	$^{22}Na^+$	Out-diffusion upstream	89	0.94 (0.84–1.03)	0.50 (0.30–0.60)
Intact	$^{22}Na^+$	Out-diffusion downstream	89	1.10 (1.0–1.20)	1.0 (0.9–1.1)
Intact	$^{22}Na^+$	Through-diffusion, incoming flux	86	0.48 (0.38–0.75)	0.47 (0.35–0.60)
Intact	$^{22}Na^+$	Through-diffusion, upstream	86	1.05–1.60	0.47–0.80
Intact	$^{22}Na^+$	Out-diffusion upstream	86	0.71 (0.60–0.78)	0.35 (0.25–0.45)
Intact	$^{22}Na^+$	Out-diffusion downstream	86	0.97 (0.88–1.06)	0.55 (0.5–0.65)
Intact	$^{22}Na^+$	Through-diffusion, incoming flux	81	0.31 (0.26–0.61)	0.28 (0.20–0.38)
Intact	$^{22}Na^+$	Through-diffusion, upstream	81	1.10–1.80	0.28–0.50
Intact	$^{22}Na^+$	Out-diffusion upstream	81	0.48 (0.44–0.52)	0.15 (0.10–0.20)
Intact	$^{22}Na^+$	Out-diffusion downstream	81	0.68 (0.61–0.76)	0.30 (0.25–0.35)

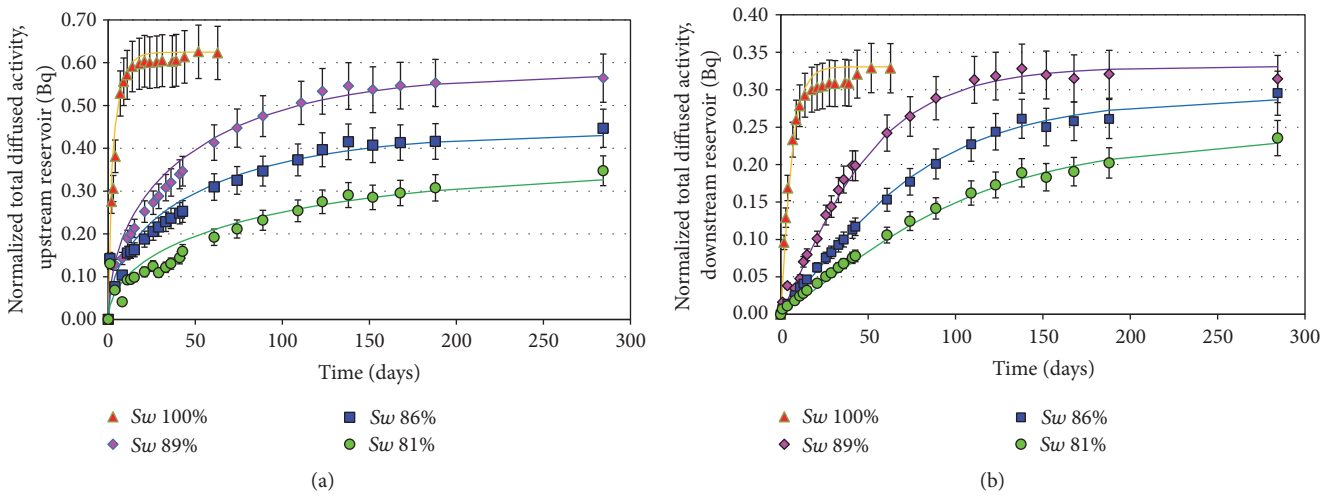

FIGURE 3: Evolution of the normalized activity in the upstream (a) and downstream (b) reservoirs of the four cells during the out-diffusion step for ^{22}Na. Decay corrections were applied with respect to the start of the through-diffusion stage. The simulated curves were calculated with the diffusive parameter values given in Table 2. The normalized activity was calculated by dividing the activity diffusing out of the sample by the total activity having diffusing in the sample during the through-diffusion experiment.

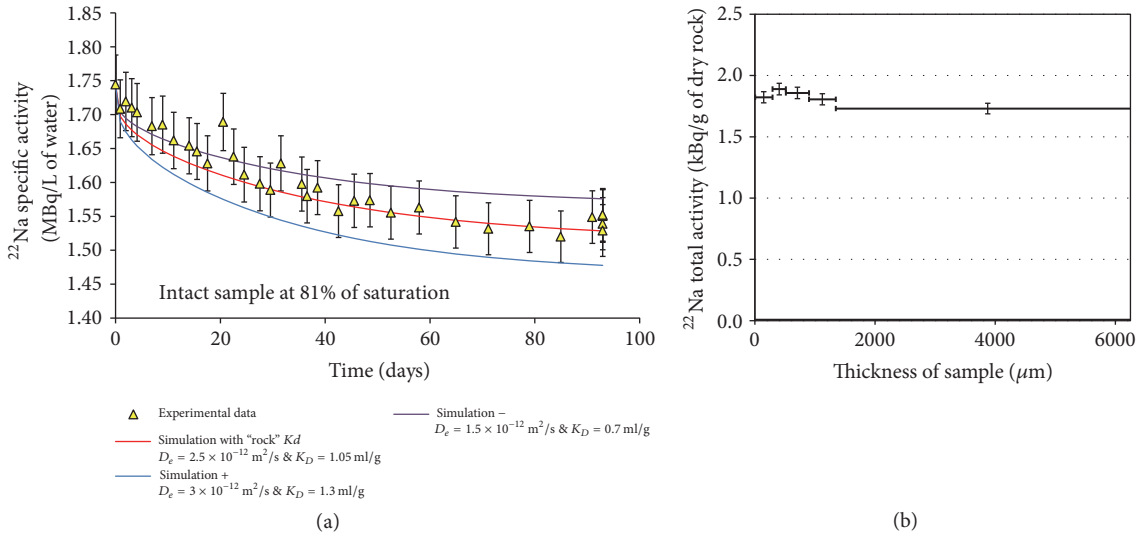

FIGURE 4: Evolution of the ^{22}Na activity in the source reservoir (a) and ^{22}Na activity profile in the intact COx sample at 81% of water saturation degree (b).

of the samples. One must note that no such discrepancy between upstream and downstream reservoirs had been observed when tritiated water or $^{125}I^-$ diffused through partially saturated COx samples [13].

We also performed a fitting approach that was based on activity decrease in upstream reservoir. However, this approach led to larger uncertainty range on diffusive parameters as compared to the ones based on the incoming flux. Indeed, the former approach only enables an estimation of the apparent diffusion coefficient (D_a) defined as D_e/α. In order to properly constrain α values and thus to obtain a better adjustment of corresponding K_D values derived from interpretation of activity decrease, two extreme cases were considered for D_e values: (i) D_e was assumed as an input parameter with its value derived from the downstream modelling (dotted line) and (ii) D_e value was adjusted to prevent the simulated incoming flux from being higher than the experimental one (dashed line). The estimated D_e and K_D values calculated from the relationship $K_D = (\alpha - \theta)/\rho_d$ are reported in Table 2. In order to well reproduce activity decrease in upstream reservoir, higher K_D values than those estimated from interpretation of the incoming flux in downstream reservoir were necessary for all these simulations (Table 2). However, independently of the two

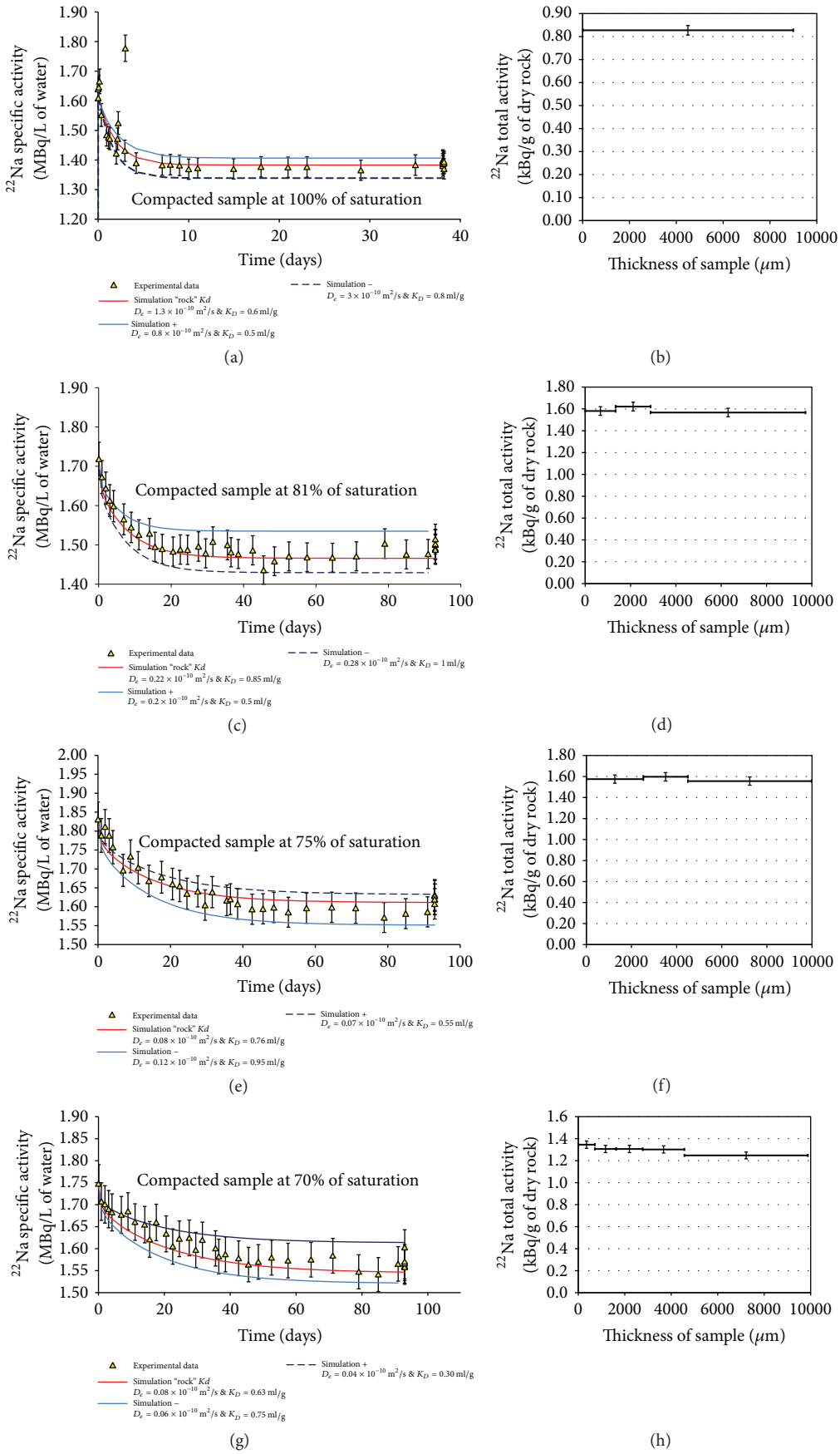

FIGURE 5: Evolution of the ^{22}Na activity in the source reservoir (a, c, e, and g) and ^{22}Na activity profiles in the four compacted COx samples (b, d, f, and h).

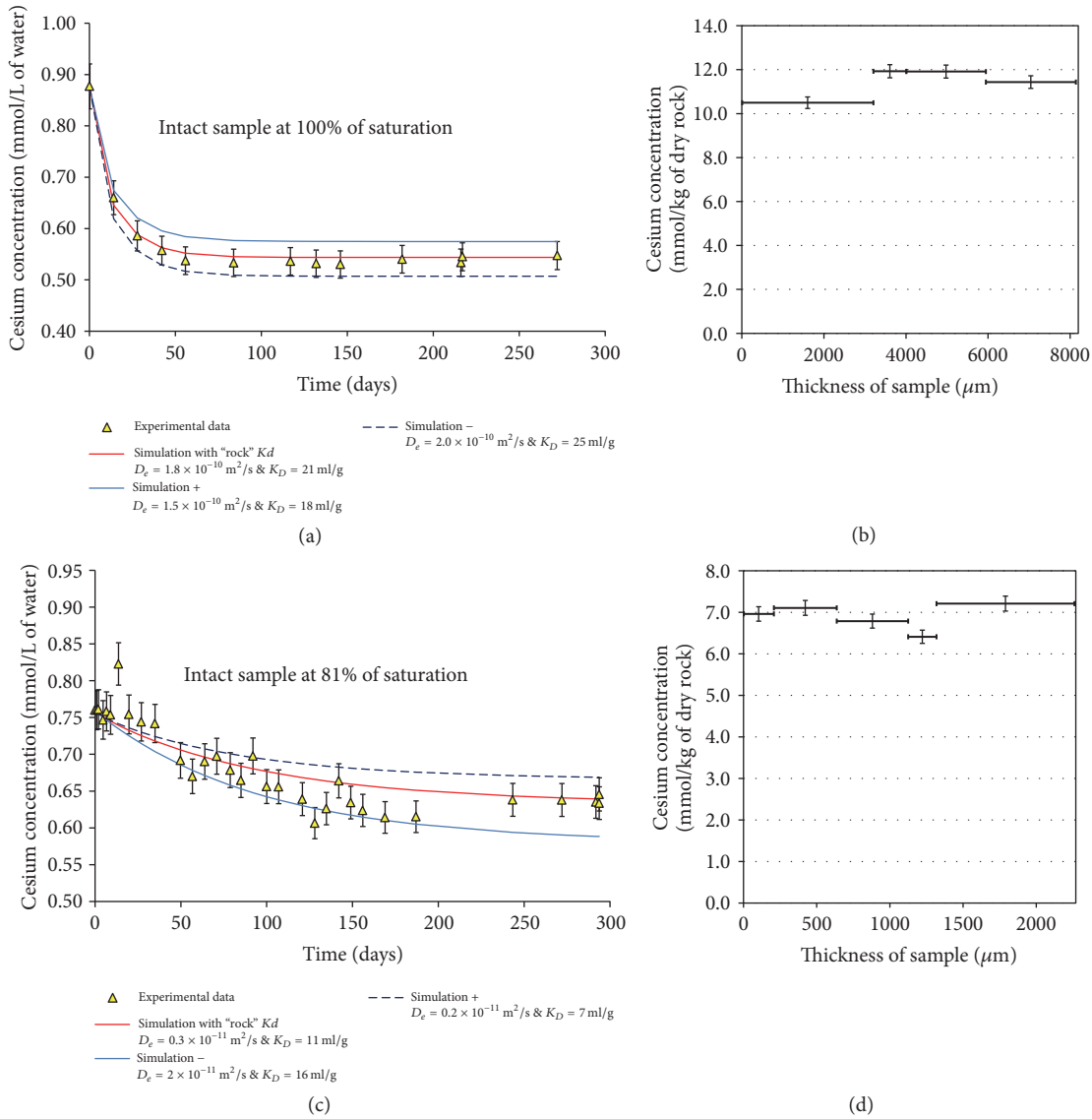

FIGURE 6: Evolution of the cesium concentration in the source reservoir (a and c) and cesium concentration profiles (b and d) in the two intact COx samples at full saturation and at 81% of saturation.

cases considered for D_e values, all these simulations failed to properly reproduce the experimental incoming flux in downstream reservoir, by underestimating these experimental data (Figure 2).

Regarding out-diffusion experiment results, the evolution of normalized total diffused activity measured in upstream and downstream reservoirs is reported in Figure 3. This normalization consists of dividing the total diffused activity by the activity that had diffused into samples during the through-diffusion step. Therefore, such approach allows the estimation of the capacity of the out-diffusion step to recover initially injected activity at the beginning of through-diffusion step. It is noteworthy that the higher desaturation is, the smaller the recovering rate is. For sample with saturation degree equal to 86% the activity recovery was less than 60% (~25% and ~35% in downstream and upstream reservoirs, resp.). This recovery was far less than full saturation, where almost 100% activity was recovered (~35% and 65% in downstream and upstream reservoirs, resp.). However, almost after 300 days of experiment, still some ^{22}Na diffused out the samples at 86% and 89% of saturation, since no plateau was yet reached. Thus it means that a longer time would be required to recover the whole activity. The associated simulated curves were calculated using (7) with the diffusive parameter values given in Table 2. The D_e values estimated from out-diffusion experiments are consistent with those estimated by analysis of the incoming flux for through-diffusion experiments (Table 2), especially those derived from the downstream data.

The results obtained from "in-diffusion until equilibrium" experiment carried out on intact clay rock sample at 81% of saturation are reported in Figures 4(a) and 4(b). Figure 4(a)

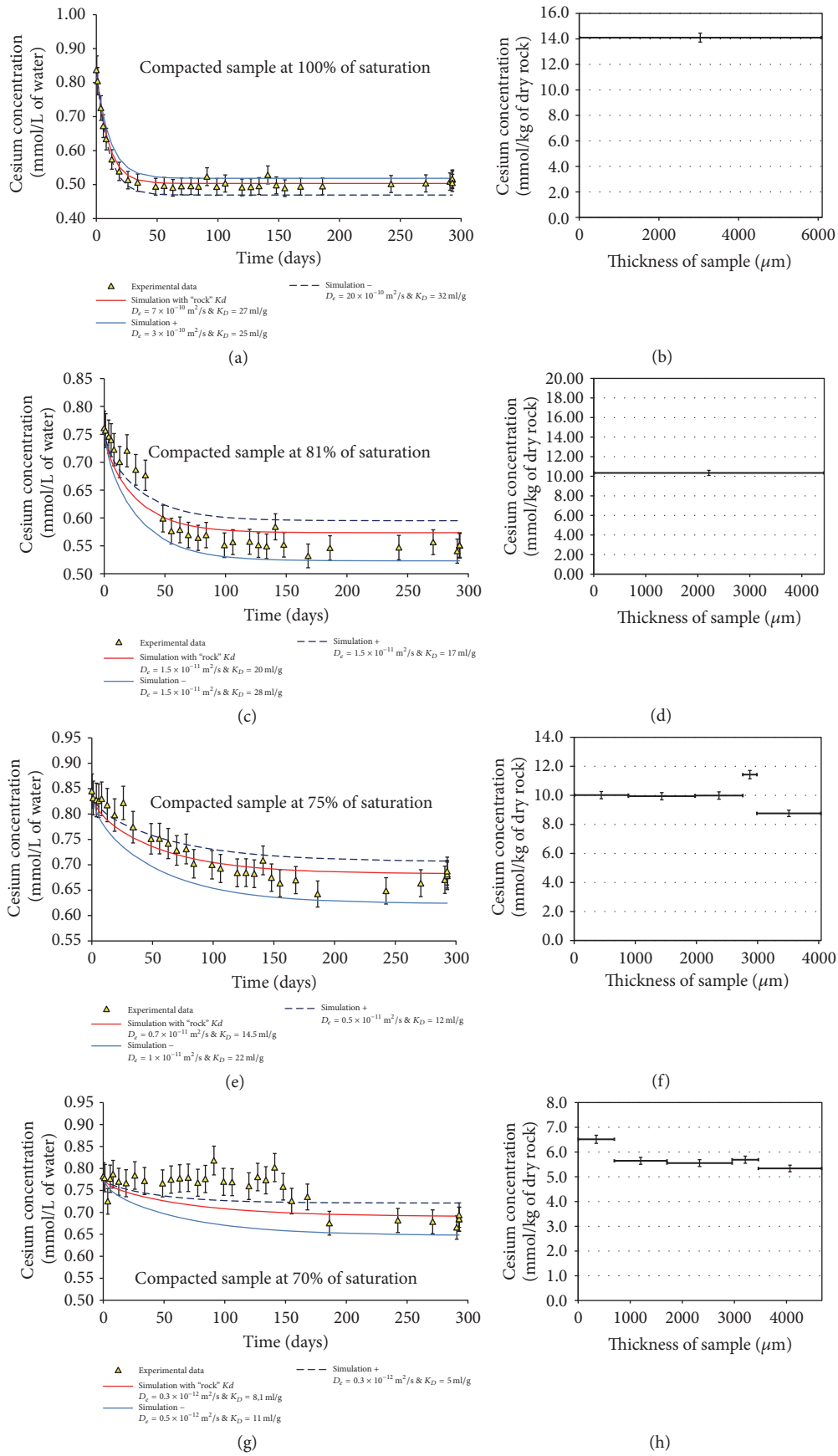

Figure 7: Evolution of the cesium concentration in the source reservoir (a, c, e, and g) and cesium concentration profile (b, d, f, and h) in the four compacted COx samples.

Table 3: Values of distribution coefficient (K_D) and effective diffusion coefficient (D_e) for the in-diffusion until equilibrium of ^{22}Na and cesium for various imposed suction values on intact and compacted materials. Values between brackets indicate the uncertainty ranges.

Sample state	Species	Saturation degree (%)	K_D (mL g^{-1})	$D_e \times 10^{-11}$(m^2 s^{-1})	[Cs] at the end of experiment (mmol L^{-1} of pure water)
Intact	$^{22}Na^+$	81	1.05 (0.70–1.30)		
Compacted	$^{22}Na^+$	100	0.60 (0.50–0.8)	13.0 (8.0–30.0)	
Compacted	$^{22}Na^+$	81	0.85 (0.50–1.00)		
Compacted	$^{22}Na^+$	75.5	0.76 (0.55–0.95)		
Compacted	$^{22}Na^+$	70	0.63 (0.30–0.75)		
Intact	^{134}Cs + [Cs]	100	21 (18–25)	18 (15–20)	0.54
Intact	^{134}Cs + [Cs]	81	11 (7–16)		0.635
Compacted	^{134}Cs + [Cs]	100	27 (25–32)	70 (30–200)	0.50
Compacted	^{134}Cs + [Cs]	81	20 (17–28)		0.55
Compacted	^{134}Cs + [Cs]	75.5	14.5 (12–22)		0.685
Compacted	^{134}Cs + [Cs]	70	8.1 (5–11)		0.690

shows ^{22}Na specific activity evolution in source reservoir as a function of time with the associated modelled curves. The ^{22}Na rock profile activity is given in Figure 4(b). By means of this ^{22}Na rock profile activity and the last measured specific activity in solution, it is possible to use (8) to directly estimate the K_D value, given in Table 3. Note that in (8), C_{solid} corresponds to the concentration of adsorbed ^{22}Na on solid, excluding ^{22}Na activity remaining in pore water. Using this "rock" K_D value, a rough modelling of activity evolution in solution can be performed using D_e values given in Figures 4(a) and 4(b). However, as mentioned above, the viscous behavior of PEG solutions prevents us from discussing more details in this part.

Figures 5(a)–5(d) show the results of "in-diffusion until equilibrium" experiments carried out on compacted clay samples at four different water saturation states. As for the intact sample, K_D values were estimated from (8) using ^{22}Na rock profile data and the last activity measurements in solution. The use of these values for modelling the activity evolution over time in solution (red line in Figures 5(a), 5(c), 5(e), and 5(g)) allowed the experimental data to be well reproduced. Note that, independently of the water saturation degree, the equilibrium state is reached in samples, even though the higher the desaturation is, the longer the time necessary to reach a plateau in solution is.

3.3. Cesium In-Diffusion Experiments. Results obtained from "in-diffusion until equilibrium" experiments on intact rock samples at full saturation and at 81% of saturation were reported in Figures 6(a)–6(d). The associated simulated curves in the figure were calculated using diffusive parameters that are directly presented in Figures 6(a) and 6(c) and also in Table 3. While the cesium concentration evolves very regularly at full saturation (Figure 6(a)), more spreading data were acquired at 81% of saturation (Figure 6(c)). However, a good consistency is revealed between Cs rock profile and the Cs concentration in solution.

Lastly, Figures 7(a)–7(h) show in-diffusion results for compacted samples at four different water saturation states along with the associated simulations. As for "in-diffusion until equilibrium" experiments on intact rocks, the presence of PEG in solution led to more spreading of ^{134}Cs activity data, especially for more concentrated one, at 70% of saturation, which exhibits no activity decrease in solution for the first 170 days and then a rapid drop until a plateau is reached (Figure 7(g)). Such results from this last experiment at 70% of saturation have to be considered cautiously, like the associated modelling.

4. Discussion

4.1. Saturation Effect on ^{22}Na Adsorption Behavior. All the K_D values estimated from through-, out-, and "in-diffusion until equilibrium" experiments on intact and compacted samples are plotted in Figure 8 as a function of water saturation degree of clay sample. At full saturation, all of the methods led to consistent dataset, taking into account associated uncertainty bars. Indeed, K_D values ranged from 0.6 mL g^{-1} for compacted sample to 0.8 mL g^{-1} for the intact sample using through-diffusion technique.

Moreover, for intact rock samples submitted to through-diffusion technique, the higher the desaturation is, the larger the discrepancy between K_D values, estimated from incoming flux in downstream reservoir and from activity decrease in upstream reservoir, is. Such a tendency can originate from the fact that K_D values from the incoming flux are estimated from the transient part of experiments. Thus these values would only reflect the ^{22}Na that are able to cross samples during this short period. The effect of saturation on these K_D values suggests that stronger the desaturation is, the more complex the diffusive pathway is, which is associated with a possible creation of dead-end pores or water films that are almost isolated from pore network, being capable of strongly slowing down the diffusion of ^{22}Na across samples. On the contrary,

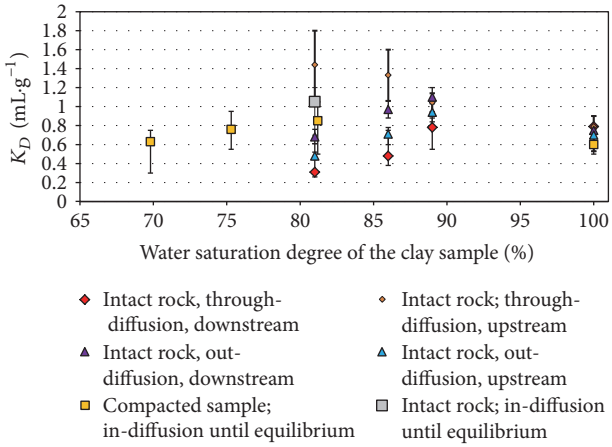

FIGURE 8: Comparison of K_D values for ^{22}Na determined on intact and compacted materials from through-, out-, and in-diffusion methods as a function of the water saturation degree of the clay sample.

K_D values estimated from upstream reservoir would probe the total amount of ^{22}Na diffusing into samples.

In-diffusion experiment carried out until equilibrium on intact rock sample at 81% of saturation led to a K_D value well matching the lowest part of large K_D range estimated from upstream data evolution during through-diffusion experiment, strengthening these previous estimations (Figure 8). Comparison of K_D values estimated from out-diffusion experiments with the ones derived from through-diffusion reveals that, at 89% of saturation, out-diffusion K_D values are close to the value estimated from upstream data during through-diffusion experiment. This observation indicates that all of the injected ^{22}Na during the through-diffusion step could be recovered by out-diffusion step. At 86% and 81% of saturation, the K_D values derived from out-diffusion are located in Figure 8 between those derived from upstream data and in-diffusion and those estimated from incoming flux during through-diffusion experiments. Thus, it suggests that time spent for out-diffusion step was not long enough to recover all ^{22}Na that diffused into these samples during the through-diffusion step (^{22}Na remaining into dead-end pores or interlayer space or near isolated water films) or there exist some processes preventing all ^{22}Na from diffusing out.

A final issue that needs to be addressed is: "how some K_D values estimated on partially saturated samples could be higher than the ones obtained at full saturation?" Could this observation have resulted due to the effect of underestimated uncertainties or of actual processes, such as an overconcentration of the pore water chemistry under partially saturated conditions due to dehydration? For the moment, this issue is still under debate.

Regarding K_D values estimated from in-diffusion on compacted samples, the saturation effect seems to be relatively low, with K_D values ranging from 0.6 mL g^{-1} at full saturation to 0.85 mL g^{-1} at 81% of saturation. Given the associated uncertainty bars, one cannot state any influence of desaturation.

To summarize, all of these results indicate that different methods used for estimating K_D values do not probe the same ^{22}Na diffusive fractions.

(i) Through-diffusion method using the incoming flux (downstream reservoir) points out that the ^{22}Na was capable of crossing samples at the beginning of experiments, giving access to the most dominant or the fastest diffusive process, which would take place in most of the connected pores.

(ii) Through-diffusion method using the activity decrease in upstream reservoir only allows an estimation of all ^{22}Na diffusing into samples.

(iii) Out-diffusion method would bring information about ^{22}Na capable of diffusing out of samples, that is, the more mobile ^{22}Na fraction.

(iv) The "in-diffusion until equilibrium" method associated with postmortem rock profile is a more accurate technique than through-diffusion using activity decrease to determine the exact amount of adsorbed ^{22}Na without any distinction between fast or slow diffusive fractions.

4.2. Saturation Effect on Cesium Adsorption Behavior. The cesium K_D values estimated in current study were compared in Figure 9 with cesium K_D values derived from Savoye et al. [14] as a function of water saturation degree of the clay sample. The previous study was performed using osmotic technique on intact partially saturated samples originated from a neighbor core. Contrary to current diffusion approach, a transient in-diffusion method had been applied for 37 days, followed by a postmortem analysis enabling the acquisition of cesium rock profiles. Both types of data (concentration decrease in solution and rock profile) had been used for determining diffusive parameters, including K_D. Note that the transient in-diffusion method used by Savoye et al. [14] led to K_D values with larger uncertainties, since α and D_e were not adjusted independently, contrary to "in-diffusion until equilibrium" method (see below).

The Savoye et al.'s [14] results did not show any clear impact of saturation on cesium adsorption (Figure 9). However, the K_D values derived in the present study for both intact and compacted samples decreased with decrease of saturation degree. However, such apparent contradiction can be related to the nonlinear behavior of cesium adsorption. Indeed, plotting all of these K_D data as a function of their associated cesium concentrations in solution at equilibrium reveals that the higher the cesium concentration in solution is, the lower the K_D values are (Figure 10), as already shown by Chen et al. [19] on fully saturated intact or compacted samples originated from the Callovo-Oxfordian formation. This suggests that nonlinear cesium adsorption could be also responsible for the main features shown in Figure 9. Finally, intact and compacted samples would behave in the same manner, with an extent of saturation effect on cesium adsorption that cannot be clearly distinguished from the nonlinear adsorption cesium behavior effect.

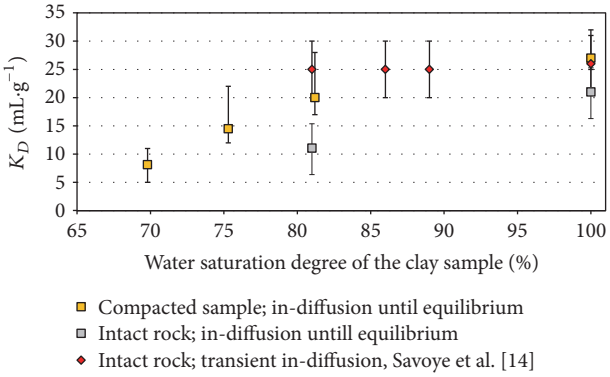

FIGURE 9: Comparison of K_D values for cesium determined on intact and compacted materials from transient in-diffusion and in-diffusion until equilibrium methods as a function of the water saturation degree of the clay sample.

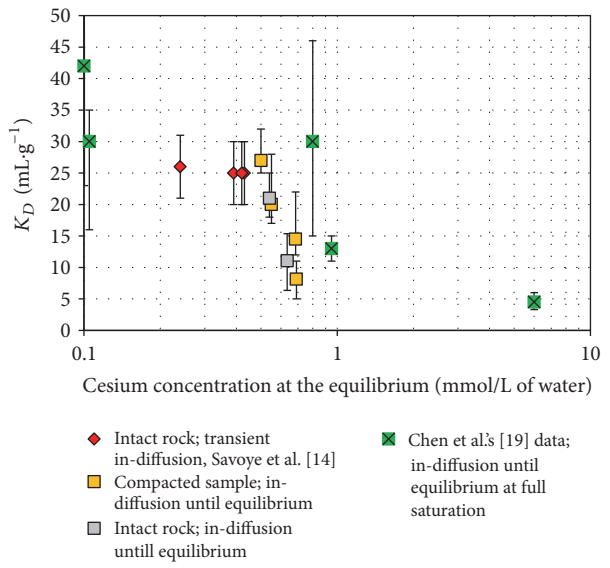

FIGURE 10: Evolution of the K_D values for cesium as a function of the associated cesium concentration in solution at the equilibrium.

4.3. Saturation Effect on Cation Diffusivity. Figure 11 shows the evolution of the diffusivity, that is, the ratio $D_e^{\text{species}}/D_w^{\text{species}}$ of each species as a function of water saturation degree of clay sample, with D_w^{species} being the diffusion coefficient in free water. HTO and cesium data derived from Savoye et al. [13] and Savoye et al. [14], respectively, on neighbor intact COx rock samples were also reported for comparison. Enhanced diffusion of cations was generally described as regards the diffusivity of HTO (used as a reference) in the same sample, according to $A = (D_e/D_w)_{\text{cations}}/(D_e/D_w)_{\text{HTO}}$.

At full saturation, on intact samples, this graph clearly highlights the enhanced diffusion for two cations with respect to tritiated water (HTO), with A being equal to 4 and 10 for sodium and cesium, respectively. This tendency was already fully documented in literature in the same Callovo-Oxfordian formation [7, 14, 16, 17, 32] but also in other argillaceous rocks [18, 21, 35]. Melkior et al. [17] found that the respective diffusivity of alkaline cations in COx is the following: Cs > Rb > K > Na > Li, as found in the present study. Enhanced diffusion for cations is also effective in compacted COx materials (ρ_d = 1.6 g cm^{-3}) under fully saturated conditions with cesium diffusivity 4 times higher than sodium one. This increased solute flux was often attributed to surface diffusion, that is, transfer of cations located in the vicinity of charged surfaces of clay particles, in the diffuse layer or even the "adsorbed" one [18]. Relationships based on nanoscale processes were proposed to explain the macroscopic behavior of cations. Based on an experimental set of K_D and D_e data, Gimmi and Kosakowski [18] have proposed an empirical relationship linking adsorption and diffusive behavior of cations, assuming there is only a fraction of cation located in diffuse layer which is capable of diffusing. They introduced a parameter, called relative diffusive mobility, μs, so as to propose the relationship between A and K_D, as follows:

$$A = 1 + \rho_d K_D \frac{\mu_s}{\varepsilon_{\text{HTO}}}. \tag{10}$$

The application of this relationship to our data, obtained on fully saturated intact samples, led to an estimation of μ_s equal to 0.29 for sodium and 0.027 for cesium. These values are very consistent with those estimated by Gimmi and Kosakowski [18] from an analysis of a large dataset acquired from sodium or cesium diffusion experiments on clay and claystones. Indeed, they estimated for sodium a μ_s median value of 0.45, with minimum and maximum values of 0.07 and 0.8, and for cesium a μ_s median value of 0.026, with minimum and maximum values of 0.005 and 0.05. Such high average surface mobility for ^{22}Na (i.e., almost 1/3 of the mobility in bulk water) can be related to the fact that adsorbed Na cations are known to be located further away from the surfaces because of their high hydration energy. Conversely, the lower average surface mobility of cesium cations can be related to their lower hydration energy and higher affinity and thus a lower probability of a movement along the clay surface [18, 36–38].

When dehydrating intact clay samples are under suction of 1.9 MPa, cesium diffusivity exhibits higher reduction (by a factor of 17) with respect to fully saturated conditions than (i) sodium diffusivity (reduction by factors of 5.1) and (ii) HTO diffusivity (reduction by a factor of 2.8) (Figure 11). However, at suction of 1.9 MPa, the sharp diffusivity reductions for cesium and, to a lesser extent, sodium are not accompanied by any decrease of the associated K_D values as initially expected (Figures 8 and 9). The application of (10), using the same μ_s values as calculated at full saturation and HTO diffusive data, led to overestimated theoretical values of D_e^{cation} at 1.9 MPa for intact state, that is, 2 and 6 times higher than the measured ones for sodium and cesium, respectively. In this case, K_D values required to estimate the correct D_e^{cation} values at 1.9 MPa from (10) should be equal to 0.3 mL g^{-1} and 1.5 mL g^{-1}, which are considerably smaller than the ones experimentally determined, that is, 0.78 mL g^{-1} and 25 mL g^{-1} for sodium and cesium, respectively.

Therefore, these results allow one to clarify the issue of the differential evolution of diffusivity for HTO and cesium

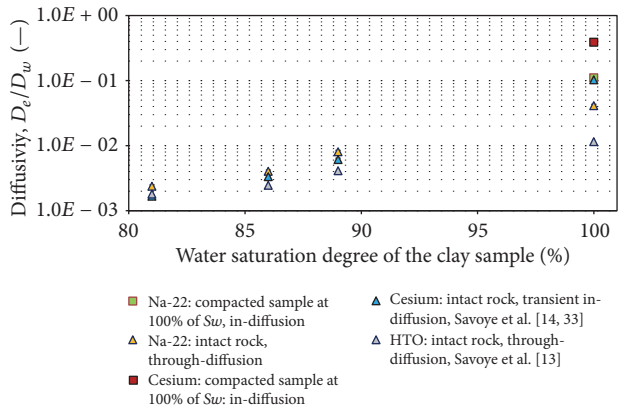

Figure 11: Diffusivity values for cesium and ^{22}Na and as a function of the water saturation degree.

as a function of saturation, raised by Savoye et al. [14]. Indeed, the distinct diffusivity reduction observed between the three species (i.e., cesium, sodium, and HTO) showed that the hypothesis suggesting that HTO would be solely responsible for differential evolution due to some evapoconcentration processes was not valid. Thus, in this case, cesium and sodium diffusivity should have similarly behaved when dehydrating, contrary to what observed. Moreover, the other hypothesis assuming that differential evolution would be due to a reduction of clay surface accessibility to cations and then a reduction of the amount of adsorbed cations when dehydrating is also largely questionable, because of the nonsignificant change of K_D values when dehydrating.

In fact, the distinct diffusivity evolution between sodium and cesium when dehydrating could be related to exacerbation of differences in their diffusive behaviors still existing at full saturation. Rotenberg et al. [37] using molecular modelling simulations demonstrated that for cation interactions with clay surface, at full saturation state, the Cs trajectories exhibited site-to-site diffusion with very localized Cs fixation sites. However, for Na, this motion is more diffuse, associated with outer-sphere Na complexes. The simulations in this study qualitatively showed the reason behind higher relative diffusive mobility, μs, of sodium compared to cesium. Moreover, using molecular modelling approach, Churakov [38] pointed out distinct evolution with saturation of different surface complexes for Na and Cs formed on montmorillonite surface. In the range of the suction values investigated in the current study, that is, from 0 MPa to 39 MPa (NaCl saline solution), his simulations indicated that Na ions mainly formed outer-sphere complexes, while the proportion of outer and inner-sphere Cs complexes calculated at full saturation (2/3 & 1/3) progressively moved to 1/3 of outer-sphere complexes and 2/3 of inner-sphere complexes. Such evolution was associated with a reduction of the distance of Cs to the clay surface, leading to a possible decrease of its relative diffusive mobility with respect to that of Na, when dehydrating. At the end, this molecular modelling study and our experimental work clearly indicate the evolutionary behavior of the relative diffusive mobility, μs, of Na and Cs according to saturation and, thus, some significant changes of double layer properties when dehydrating.

5. Summary and Conclusion

The diffusion and adsorption properties of ^{22}Na and cesium have been investigated on fully saturated and partially saturated core of Callovo-Oxfordian (COx) claystones. Through-, out-, and in-diffusion laboratory experiments have been performed on intact or compacted samples partially saturated using the osmotic method for imposed suction up to 9 MPa. The aim was to address the issue of the unexpected differential evolution of diffusivity for the tritiated water (HTO) and cesium as a function of saturation, raised by Savoye et al. [14] in intact neighbor COx samples. The problem was approached by (i) adapting a method developed at full saturation to partially water-saturated conditions in order to properly determine K_D value on intact or compacted samples and (ii) studying a third species, the sodium, expected to behave in an intermediate manner between cesium and HTO. The main findings and conclusion were as follows:

(1) The application of suction up to 9 MPa allowed intact samples to be dehydrated down to 81% and compacted samples down to 70%. Moreover, at each suction level strictly higher than 0 MPa, compacted materials displayed saturation degree values about 10% lower as compared to the ones measured on intact materials.

(2) At full saturation, a good consistency was evidenced between the K_D values estimated on intact and compacted samples for ^{22}Na and Cs, in accordance with previous studies such as the one carried out by Chen et al. [19] for cesium.

(3) Independently of sample state (intact or compacted), one cannot conclude whether desaturation drastically impacted ^{22}Na adsorption, given the associated uncertainty bars. However, in detail, some epiphenomena were revealed depending on the diffusion methods used for determining K_D values. The through-diffusion method using the incoming flux would point out ^{22}Na capable of crossing samples in the beginning of the experiments, giving access to the most dominant or the fastest diffusive process; the out-diffusion method would bring information

about ^{22}Na capable of diffusing out of samples, that is, the more mobile ^{22}Na fraction; the "in-diffusion until equilibrium" associated with postmortem rock profile enabled the determination of the exact amount of adsorbed ^{22}Na, without any distinction between fast and slow ^{22}Na diffusive fractions.

(4) For cesium, intact and compacted samples would similarly behave, with an extent of saturation effect on cesium adsorption that cannot be clearly distinguished from the dependence of cesium sorption to cesium concentration in pore water.

(5) Therefore, very small impact of saturation on the extent of adsorption for ^{22}Na and cesium would indicate that the saturation degrees were not low enough to limit the access of cations to clay surfaces (including interlayer space) onto which they could be adsorbed. Clay matrix was unlikely emptied by the highest suction values used in this study.

(6) At full saturation, enhanced diffusion for ^{22}Na and cesium was clearly evidenced on intact samples with diffusivity 4 and 10 times higher than that of tritiated water (HTO), respectively, in accordance with previous works. Even though no HTO data were acquired on compacted samples, the very large diffusivity of cesium estimated on these types of material, that is, 4 times higher than that measured for ^{22}Na, clearly showed that enhanced diffusion would also take place in such compacted materials.

(7) When dehydrating clay samples, the diffusion was clearly slower than that in fully saturated samples. Diffusivity for cesium decreased, from 0 to 1.9 MPa of suction, by a factor of 17 and for sodium by a factor of 5 for intact materials. The distinct diffusivity reduction observed between each species and the nonsignificant change of K_D values showed the role played by desaturation for exacerbating differences in diffusive behaviors of cesium, sodium, and HTO. A differential decrease of the relative diffusive mobility in diffuse layer of adsorbed cesium compared to adsorbed sodium was then proposed based on a literature review, in addition to the particular behavior of HTO, which could diffuse both in liquid and gaseous phases so as to reduce its diffusive pathways.

Conflicts of Interest

The authors declare that they have no conflicts of interest.

Acknowledgments

The work focusing on the ^{22}Na through- and out-diffusion experiments on intact rocks received financial support from Andra and CEA, while the part dedicated to in-diffusion experiments received financial support from Andra. We gratefully acknowledge A. Rajyaguru for English improvement.

References

[1] Andra, "Dossier 2005 argile – Tome – Evolution phénoménologique du stockage géologique," Rapport Andra no. C.RP.ADS .04.0025, France, http://www.andsite-principal/document/editions/182.pdf, 2005.

[2] M. J. Hendry, D. K. Solomon, M. Person et al., "Can argillaceous formations isolate nuclear waste? Insights from isotopic, noble gas, and geochemical profiles," *Geofluids*, vol. 15, no. 3, pp. 381–386, 2015.

[3] S. G. Fityus, D. W. Smith, and J. R. Booker, "Contaminant transport through an unsaturated soil liner beneath a landfill," *Canadian Geotechnical Journal*, vol. 36, no. 2, pp. 330–354, 1999.

[4] G. Armand, F. Leveau, C. Nussbaum et al., "Geometry and properties of the excavation-induced fractures at the meuse/haute-marne URL drifts," *Rock Mechanics and Rock Engineering*, vol. 47, no. 1, pp. 21–41, 2014.

[5] P. Marschall, S. Horseman, and T. Gimmi, "Characterisation of gas transport properties of the Opalinus Clay, a potential host rock formation for radioactive waste disposal," *Oil & Gas Science and Technology - Revue d'IFP Energies nouvelles*, vol. 60, no. 1, pp. 121–139, 2005.

[6] L. R. Van Loon, J. M. Soler, W. Müller, and M. H. Bradbury, "Anisotropic diffusion in layered argillaceous rocks: A case study with Opalinus Clay," *Environmental Science & Technology*, vol. 38, no. 21, pp. 5721–5728, 2004.

[7] S. Savoye, C. Beaucaire, B. Grenut, and A. Fayette, "Impact of the solution ionic strength on strontium diffusion through the Callovo-Oxfordian clayrocks: An experimental and modeling study," *Applied Geochemistry*, vol. 61, pp. 41–52, 2015.

[8] C. E. Schaefer, R. R. Arands, H. A. van der Sloot, and D. S. Kosson, "Prediction and experimental validation of liquid-phase diffusion resistance in unsaturated soils," *Journal of Contaminant Hydrology*, vol. 20, no. 1-2, pp. 145–166, 1995.

[9] S. Hamamoto, M. Samintha Anne Perera, A. Resurreccion et al., "The solute diffusion coefficient in variably compacted, unsaturated volcanic ash soils," *Vadose Zone Journal*, vol. 8, no. 4, pp. 942–952, 2009.

[10] D. Aldaba, A. Rigol, and M. Vidal, "Diffusion experiments for estimating radiocesium and radiostrontium sorption in unsaturated soils from Spain: Comparison with batch sorption data," *Journal of Hazardous Materials*, vol. 181, no. 1-3, pp. 1072–1079, 2010.

[11] T. K. Tokunaga, S. Finsterle, Y. Kim, J. Wan, A. Lanzirotti, and M. Newville, "Ion Diffusion Within Water Films in Unsaturated Porous Media," *Environmental Science & Technology*, vol. 51, no. 8, pp. 4338–4346, 2017.

[12] C. D. Shackelford, "Laboratory diffusion testing for waste disposal - A review," *Journal of Contaminant Hydrology*, vol. 7, no. 3, pp. 177–217, 1991.

[13] S. Savoye, J. Page, C. Puente, C. Imbert, and D. Coelho, "New experimental approach for studying diffusion through an intact and unsaturated medium: A case study with callovo-oxfordian argillite," *Environmental Science & Technology*, vol. 44, no. 10, pp. 3698–3704, 2010.

[14] S. Savoye, C. Beaucaire, A. Fayette, M. Herbette, and D. Coelho, "Mobility of cesium through the callovo-oxfordian claystones under partially saturated conditions," *Environmental Science & Technology*, vol. 46, no. 5, pp. 2633–2641, 2012.

[15] S. Savoye, C. Imbert, A. Fayette, and D. Coelho, "Experimental study on diffusion of tritiated water and anions under variable water-saturation and clay mineral content: Comparison with

the Callovo-Oxfordian claystones," *Geological Society, London, Special Publications*, vol. 400, no. 1, pp. 579–588, 2014.

[16] T. Melkior, S. Yahiaoui, S. Motellier, D. Thoby, and E. Tevissen, "Cesium sorption and diffusion in Bure mudrock samples," *Applied Clay Science*, vol. 29, no. 3-4, pp. 172–186, 2005.

[17] T. Melkior, S. Yahiaoui, D. Thoby, S. Motellier, and V. Barthès, "Diffusion coefficients of alkaline cations in Bure mudrock," *Physics and Chemistry of the Earth*, vol. 32, no. 1-7, pp. 453–462, 2007.

[18] T. Gimmi and G. Kosakowski, "How mobile are sorbed cations in clays and clay rocks?" *Environmental Science & Technology*, vol. 45, no. 4, pp. 1443–1449, 2011.

[19] Z. Chen, G. Montavon, S. Ribet et al., "Key factors to understand in-situ behavior of Cs in Callovo-Oxfordian clay-rock (France)," *Chemical Geology*, vol. 387, no. 1, pp. 47–58, 2014.

[20] G. Montavon, E. Alhajji, and B. Grambow, "Study of the interaction of Ni2+ and Cs+ on MX-80 bentonite; effect of compaction using the "capillary method"," *Environmental Science & Technology*, vol. 40, no. 15, pp. 4672–4679, 2006.

[21] L. R. Van Loon and J. Eikenberg, "A high-resolution abrasive method for determining diffusion profiles of sorbing radionuclides in dense argillaceous rocks," *Applied Radiation and Isotopes*, vol. 63, no. 1, pp. 11–21, 2005.

[22] E. Gaucher, C. Robelin, J. M. Matray et al., "ANDRA underground research laboratory: Interpretation of the mineralogical and geochemical data acquired in the Callovian-Oxfordian formation by investigative drilling," *Physics and Chemistry of the Earth*, vol. 29, no. 1, pp. 55–77, 2004.

[23] P. Delage, M. D. Howat, and Y. J. Cui, "The relationship between suction and swelling properties in a heavily compacted unsaturated clay," *Engineering Geology*, vol. 50, no. 1-2, pp. 31–48, 1998.

[24] A. Vinsot, S. Mettler, and S. Wechner, "In situ characterization of the Callovo-Oxfordian pore water composition," *Physics and Chemistry of the Earth*, vol. 33, no. 1, pp. S75–S86, 2008.

[25] S. Altmann, M. Aertsens, T. Appelo et al., "Processes of cation migration in clayrocks," Final Scientific Report CEA-R-6410, p. 143, 2015.

[26] S. Savoye, J.-L. Michelot, F. Bensenouci, J.-M. Matray, and J. Cabrera, "Transfers through argillaceous rocks over large space and time scales: Insights given by water stable isotopes," *Physics and Chemistry of the Earth*, vol. 33, no. 1, pp. S67–S74, 2008.

[27] S. Savoye, J.-L. Michelot, C. Wittebroodt, and M. V. Altinier, "Contribution of the diffusive exchange method to the characterization of pore-water in consolidated argillaceous rocks," *Journal of Contaminant Hydrology*, vol. 86, no. 1-2, pp. 87–104, 2006.

[28] S. Didierjean, D. Maillet, and C. Moyne, "Analytical solutions of one-dimensional macrodispersion in stratified porous media by the quadrupole method: Convergence to an equivalent homogeneous porous medium," *Advances in Water Resources*, vol. 27, no. 6, pp. 657–667, 2004.

[29] G. J. Moridis, "A set of semi-analytical solutions for parameter estimation in diffusion cell experiments," Report LBNL-41857, Lawrence Berkeley National Laboratory, Berkeley, Calif, USA, 1998.

[30] A. Jakob, F-A. Sarott, and P. Spieler, "Diffusion and sorption on hardened cement pastes – experiments and modelling results," Paul Scherrer Institut Report, http://www.iaea.org/inis/collection/NCLCollectionStore/_Public/30/058/30058512.pdf?r=1, 1999.

[31] M. Descostes, V. Blin, F. Bazer-Bachi et al., "Diffusion of anionic species in Callovo-Oxfordian argillites and Oxfordian limestones (Meuse/Haute-Marne, France)," *Applied Geochemistry*, vol. 23, no. 4, pp. 655–677, 2008.

[32] S. Savoye, F. Goutelard, C. Beaucaire et al., "Effect of temperature on the containment properties of argillaceous rocks: The case study of Callovo-Oxfordian claystones," *Journal of Contaminant Hydrology*, vol. 125, no. 1-4, pp. 102–112, 2011.

[33] S. Savoye, B. Frasca, B. Grenut, and A. Fayette, "How mobile is iodide in the Callovo-Oxfordian claystones under experimental conditions close to the in situ ones?" *Journal of Contaminant Hydrology*, vol. 142-143, pp. 82–92, 2012.

[34] C. S. Tang, A. M. Tang, Y. J. Cui, P. Delage, C. Schroeder, and B. Shi, "A study of the hydro-mechanical behaviour of compacted crushed argillite," *Engineering Geology*, vol. 118, no. 3-4, pp. 93–103, 2011.

[35] Y. Tachi, K. Yotsuji, Y. Seida, and M. Yui, "Diffusion and sorption of Cs+, I- and HTO in samples of the argillaceous Wakkanai Formation from the Horonobe URL, Japan: Clay-based modeling approach," *Geochimica et Cosmochimica Acta*, vol. 75, no. 22, pp. 6742–6759, 2011.

[36] Y. Kim and R. J. Kirkpatrick, "23Na and 133Cs NMR study of cation adsorption on mineral surfaces: Local environments, dynamics, and effects of mixed cations," *Geochimica et Cosmochimica Acta*, vol. 61, no. 24, pp. 5199–5208, 1997.

[37] B. Rotenberg, V. Marry, J.-F. Dufrêche, N. Malikova, E. Giffaut, and P. Turq, "Modelling water and ion diffusion in clays: A multiscale approach," *Comptes Rendus Chimie*, vol. 10, no. 10-11, pp. 1108–1116, 2007.

[38] S. V. Churakov, "Mobility of Na and Cs on montmorillonite surface under partially saturated conditions," *Environmental Science & Technology*, vol. 47, no. 17, pp. 9816–9823, 2013.